

Fluid Flow Behaviors around Wedge-shaped Body using Lattice Boltzmann Method

LBM을 이용한 쐐기형 물체 주위의 유동특성

M. A. Taher, H. Y. Jung and Y. W. Lee
무하마드 아부 타헤르 · 정호윤 · 이연원

(received 1 June 2009, revised 9 July 2009, accepted 9 July 2009)

주요 용어 : Wedge-Shaped Body(쐐기형 물체), Lattice-Boltzmann Method(Lattice Boltzmann법), Strouhal Number (Strouhal 수), Vortex Shedding(와 방출)

요 약 : 본 연구에서는 기존에 널리 사용되어져 온 Navier-Stokes 방정식을 풀이하는 전통적인 CFD 해석에서 벗어나 최근에 그 응용 분야를 넓혀가고 있는 LBM의 해석코드를 개발하고, 이를 이용하여 이차원 채널 속에 놓여진 쐐기형 물체 주위의 유동특성을 조사하였다. D2Q9 격자계 및 Bhatnagar-Gross-Krook (LBGK) 모델을 채택하였으며, 수치해석 결과는 기존의 실험결과와 잘 일치하였다. 쐐기형 물체에서 와의 형성 및 방출 Reynolds 수 범위는 $32 \leq Re \leq 620$ 이며, 원형실린더에서 알려진 Karman 와열을 형성하는 주기적인 와 방출은 대칭적인 와가 형성된 후 $Re \geq 85$ 부터 시작되며 Reynolds 수의 증가에 따라 와 방출 주파수는 증가되었다.

1. 서 론

In the past years, the Lattice - Boltzmann Method (LBM) has attracted much attention as a novel alternative to traditional computational fluid dynamics (CFD) methods for numerically solving the Navier-Stokes(N-S) equation. Unlike N-S solvers, LBM does not need to solve partial differential equations and resultant algebraic equations. It only involves algebraic operation. This method is simple and easy for implementation. However, the LBM has demonstrated a significant potential and broad applicability with numerous computational advantages to incorporate microscopic interactions.

Actually LBM originated from the cellular automata (CA). A cellular automaton (CA) is used to simulate the microscopic movements and collisions in order to get the continuum

macroscopic equations of fluid dynamics in two and three dimensions. The class of cellular automata (CA) is used for the simulation of fluid dynamics. It also is called the Lattice Gas Automata (LGA), which is considered as a fictitious molecular dynamics (MD) in which space, time and particle velocities all are discrete. Lattice gas models with an appropriate choice of the lattice symmetry in fact represent numerical solutions of the N-S equations and therefore able to describe the hydrodynamic problems discussed by¹⁾. It is commonly recognized that the LBM can faithfully be used to simulate the incompressible N-S equations with high accuracy and this lattice BGK (LBGK) model. The LBGK model makes simulation more efficient and allows flexibility of the transport co-efficient, which has been derived from lattice gas automata and leads to the real N-S equations of incompressible flow under steady mass density condition by appropriate choice of the local equilibrium distribution²⁾. However, LBM is limited to the low Mach number(near incompressible) flow

이연원(책임저자) : 부경대학교 기계공학부
E-mail : ywlee@pknu.ac.kr, Tel : 051-629-6162
무하마드 아부 타헤르, 정호윤 : 부경대학교 대학원

simulation and it has been studied by Xu and He³⁾. An overview of LBM, a parallel and efficient algorithm for simulating single-phase and multiphase fluid flows and also for incorporating additional physical complexities have been discussed by Chen and Doolen⁴⁾. There is no doubt that the LBM has several advantages over other conventional CFD methods, especially dealing with complex boundaries, incorporating of microscopic interactions, are described in the excellent books^{5,6)}.

It is known that an enormous corpus of literature on the subject of bluff body wakes has developed since the pioneering work of Strouhal and Von Karman. This flow situation is popular not only because of its academic attractiveness but also owing to its related technical problems associated with energy conservation and structural design. A laminar vortex shedding region is known to occur for the Reynolds number range extending approximately from 50-80 and the universal relationship between Reynolds and Strouhal numbers around a circular cylinder have been studied by Williamson⁷⁾. The numerical formulation of laminar vortex shedding flow past a circular cylinder using coupled boundary element method (BEM) and three-step finite element method (FEM) are briefly described by Young et.al.⁸⁾. Actually many authors have been studied the vortex shedding frequency behind a circular cylinder or square cylinder or two cylinders for different cases both in numerically and experimentally⁹⁻¹¹⁾. However, in this paper, the present authors would like to investigate the fluid flow behavior around a wedge-shaped body using the lattice Boltzmann method (LBM). As far we know, the problem has been considered before. The objective of this paper is to numerically study of fluid flow behavior around wedge-shaped body where the flow can be driven with the pressure (density) gradients. Here we have focused our attention on the evolution of streamlines, vorticity contours, pressure contours as well as velocity profiles and

vortex shedding frequency, to investigate the important characteristics of the flow field around wed-shaped body, for a wide range of non-dimensional parameters, namely the Reynolds number (Re) and the Strouhal number (St), based on the characteristic length of the body, the maximum incoming flow velocity (less than $0.1lu$) and also the nature of fluid transport properties. Throughout our calculation we use the Lattice-Boltzmann units. Most LBM simulation Δx and Δt are assumed as the space and time unit respectively. The lattice unit (lu) is the fundamental measure of length and time steps (ts) is the unit of time in LBM.

2. Formulation of the Problem

The computational domain is to consider as a rectangular region $L \times H$, where H is the height of the channel and $L=4H$ is the length of the channel. A wedge-shaped body having wedge angle $\theta = 90^\circ$ is placed symmetrically between parallel walls as shown in Fig.1.

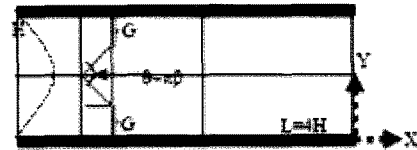


Fig. 1 Physical model and coordinate systems

Actually the wedge angle is defined by $\theta = \pi\beta$, $0 \leq \beta \leq 1$. It is noted that the case β equal to zero corresponds to flow over a flat plate while β equal to one corresponds to flow over a vertical flat plate. In an incompressible flow, Reynolds number is one of the major parameters that controls the flow field and is define by $Re=Uh/\nu$, where U and h are the characteristic velocity and the length of the bluff body respectively. If a body is placed in a flow stream, vortices form behind shed alternately from each side. A vortex can be any circular or rotary flow that possesses vorticity. Vorticity is a mathematical concept used in fluid dynamics. Mathematically, it is defined as,

$w = \nabla \times \vec{u}$, where \vec{u} is the fluid velocity. The non dimensional shedding frequency, the Strouhal number, is defined as: $St = fh/U$, where f is the vortex shedding frequency. Over a wide range of Reynolds numbers, the Strouhal number is constant, implying a linear relationship between shedding frequency and mean velocity. It is found that the Strouhal number is almost constant value of 0.2 in the Reynolds number range of $300 < Re < 2 \times 10^5$. Williamson⁷⁾ has given a least-squares fit to the universal Strouhal number curve for the low Reynolds number regime as $St = A/Re + B + CRe$, where $A = -3.3265$, $B = 0.1816$, and $C = 1.6 \times 10^{-4}$. This relation is believed to be accurate to $\pm 1\%$ in the Reynolds number. In order to simulate a fully developed laminar channel flow, a parabolic velocity profile can be expressed as

$$u(y) = U[1 - (1 - 2y/H)^2] \quad (1)$$

where U is the maximum velocity at the channel inlet. This velocity is chosen to be lower than 10% of the speed of sound for LBM simulation to avoid significant compressibility effects. At the top and bottom wall, no slip boundary conditions namely zero fluid velocity. $u = v = 0$, have been imposed by the standard bounce back rule.

In LBM, the movement of the fluid particles are modeled instead of solving directly the macroscopic fluid quantities like the velocity and the pressure. It is known as mesoscopic simulation model, which is based on the Boltzmann equation (BE). Neglecting external forces, the Boltzmann equation (BE) with BGK approximation can be defined as

$$\frac{\partial F_i}{\partial t} + \vec{e}_i \cdot \frac{\partial F_i}{\partial \vec{x}_i} = -\frac{1}{\tau} (F_i - F_i^{eq}), \quad i=0,1,\dots,q-1 \quad (2)$$

where $F_i(\vec{x}, t)$ is the discrete particle distribution function and $F_i^{eq}(\vec{x}, t)$ is the discrete equilibrium distribution function at lattice position \vec{x} and time t discussed by³⁾. The total number of

discrete particle velocities (e_i) on each node in D2Q9 model is 9. The velocities of the particles are such that they move from one node to another during each time step. These particle velocities can be written as

$$e_i = \begin{cases} (0,0) & i = 0, \\ c[\cos(\frac{i-1}{2}\pi), \sin(\frac{i-1}{2}\pi)] & i = 1,2,3,4, \\ \sqrt{2}c[\cos(\frac{i-5}{2}\pi + \frac{\pi}{4}), \sin(\frac{i-5}{2}\pi + \frac{\pi}{4})] & i = 5,6,7,8, \end{cases}$$

Here $c = \Delta x / \Delta t$ is called CFL number. Therefore the discrete form of equation (2) is called the Lattice Boltzmann equation (LBE) and can be written as

$$F_i(\vec{x} + \Delta t \vec{e}_i, t + \Delta t) - F_i(\vec{x}, t) = -\frac{1}{\tau} (F_i - F_i^{eq}) \quad (3)$$

Here $\omega = 1/\tau$ is the relaxation parameter and depends on the local macroscopic variables, ρ and, $\vec{\rho u}$ and should satisfy the following laws of conservation:

$$\rho = \sum_i F_i \quad \text{and} \quad \vec{\rho u} = \sum_i \vec{e}_i F_i \quad (4)$$

The above expressions describe the relationships between the microscaled quantities define on the basis of lattice sizes and the macroscaled physical quantities of flow such as the mass density and the velocity of the fluid. The general form of the equilibrium distribution function can be written up to $O(u^2)$ [8]

$$F_i^{eq} = \rho w_i [1 + \frac{3}{c^2} \vec{e}_i \cdot \vec{u} + \frac{9}{2c^4} (\vec{e}_i \cdot \vec{u})^2 - \frac{3}{c^2} u^2] \quad (5)$$

where w_i is the lattice weighting factors depend only on the lattice model. For D2Q9 model, $w_0 = 4/9$, $w_i = 1/9$, $i = 1, 2, 3, 4$, and $w_i = 1/36$, $i = 5, 6, 7, 8$. Using the Chapman-Enskog expansion, it is mathematically provable that the equation (3) can recover the N-S equations, if the pressure and the kinetic viscosity are presented by

$$P = \rho Cs^2 \quad \text{and} \quad \nu = (\tau - \frac{1}{2}) Cs^2 \Delta t \quad (6)$$

where the speed of sound in this model is defined by $Cs = \sqrt{RT}$. It should be noted that

the temperature T has no physical significance for the isothermal model ($T=\text{constant}$). And thus, the grid CFL number can be defined as

$$c = \sqrt{3RT} = \frac{\Delta x}{\Delta t} = 1$$

In this simulation, we consider, $\Delta x = 1lu = 6.33 \times 10^{-6} \text{m}$, $\Delta t = 1 \text{ts} = 1.15 \times 10^{-8} \text{s}$. The fluid properties are taken to air properties. The kinematic viscosity $\nu = 15.63 \times 10^{-6} \text{m}^2/\text{s}$, corresponds to 0.0045 lattice unit. All reported data are obtained on our calculation domain 320×80 (lattice node). For accurate solution, the Mach number, Ma , should be kept as small as possible. In general U in order of 0.2 or 0.1 or less. Therefore, the Reynolds number should be chosen very carefully.

3. Results and Discussions

In conventional CFD methods for incompressible N-S equations, one needs to solve the Poisson equation for the pressure. However in LBM, solving the equation (3), we get all information that we interested to simulate in our study including pressure terms. The algebraic equation (3) is the main governing equation and it is solved by uniform 2D grid system along with boundary conditions and other equations described as above.

One important quantity taken into account in the present simulation is the Strouhal number (St), computed from the height (h) of the bluff body, the vortex shedding frequency and the velocity of the incoming fluid. In order to assess the accuracy of our method, we compare our results (LBM) with other published works. As the experimental and numerical data are available only the flow around a circular cylinder or square cylinder but not available in wedge-shaped body, so we would compare our result with available results. The dimensionless shedding frequency with Reynolds numbers in the wake of circular cylinder, whose diameter is D , as shown in Fig. 2.

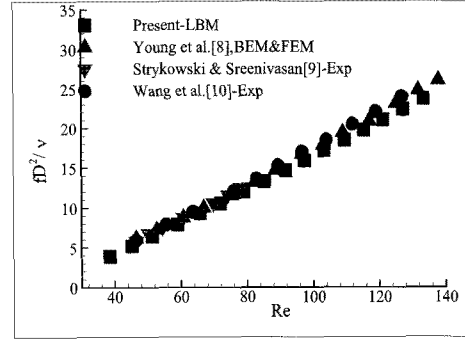


Fig. 2 Comparison of dimensionless shedding frequency with Reynolds number

The results are compared with numerical results of Young et al.⁸⁾ and experimental results of Wang et al.⁹⁾, Strykowski and Sreenivasan¹⁰⁾. It is seen a good agreement with both experimental and numerical simulations. Wang et al.⁹⁾, Strykowski and Sreenivasan¹⁰⁾ have shown in their experimental investigation the Reynolds number in the range 44-80 and 44-129 respectively. However, Young et al.⁸⁾ have found the Reynolds number in the range 44-144 by using coupled boundary element method (BEM) and three-step finite element method (FEM). Moreover, the present study indicates the Reynolds number in the range 36-138. However, the vortex shedding frequency for different bluff bodies e.g. wedge-shaped body, square cylinder and circular cylinder with Reynolds number under the conditions that described in section 2 as shown in Fig.3.

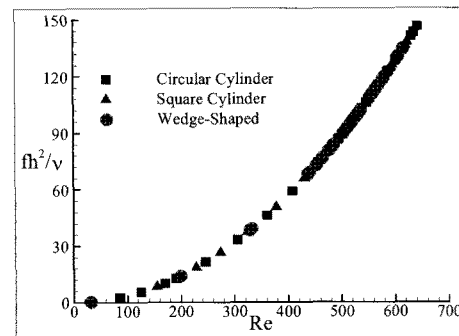


Fig. 3 Variation of dimensionless shedding frequency with Reynolds number

Fig. 3 indicates that the dimensionless vortex shedding frequency increases with the Reynolds

number. For wedge-shaped body it is found the Reynolds number in the range up to 32-620. However, for circular cylinder it is seen up to 82-650 and for square cylinder it is seen up to 150-635. The higher frequency means that the process of vortex shedding is faster. The nature of the vortex shedding is a strong function of the Re. In our simulation, a Von Karman vortex street is predicted behind the wedge-shaped body with periodicity if $Re \geq 85$. This kind of flow behavior is observed with different Re for different bodies. Under the same conditions is found at $Re \geq 120$ for circular cylinder and $Re \geq 225$ for rectangular cylinder.

A detailed view of flow field behind the wedge-shaped body and changes in the vortex shedding pattern with different Reynolds numbers can easily be observed from Fig.4.

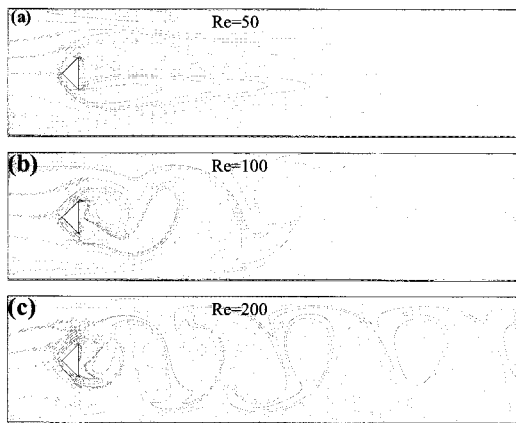


Fig. 4 Vorticity in x-y plane for different Re

In these figures the negative vorticity (clockwise vortex) is shown by dashed lines and the positive vorticity (anticlockwise vortex) by solid lines. It is seen from 4(a) that for low Reynolds number, a pair of vortices with same strength and size are formed just behind the body; a positive vortex appears on the lower part of the body and a negative vortex on the upper part of the body. Fig 4(b) and 4(c), an important change in the flow is observed for high Reynolds number ($=100, 200$). The flow behind the body is characterized by Karman vortex street, which consists of vortices in a regular

arrangement. These alternating vortices with the same strength and size are shed from the upper and lower leading edges. The distance between consecutive vortices remains almost constant. Therefore, it is clear that the Karman vortex street starts at $Re \geq 85$ for the fluid flow past a wedge-shaped body in a channel.

To analyze the time development of vorticity for $Re = 100$ is shown in Fig.5.

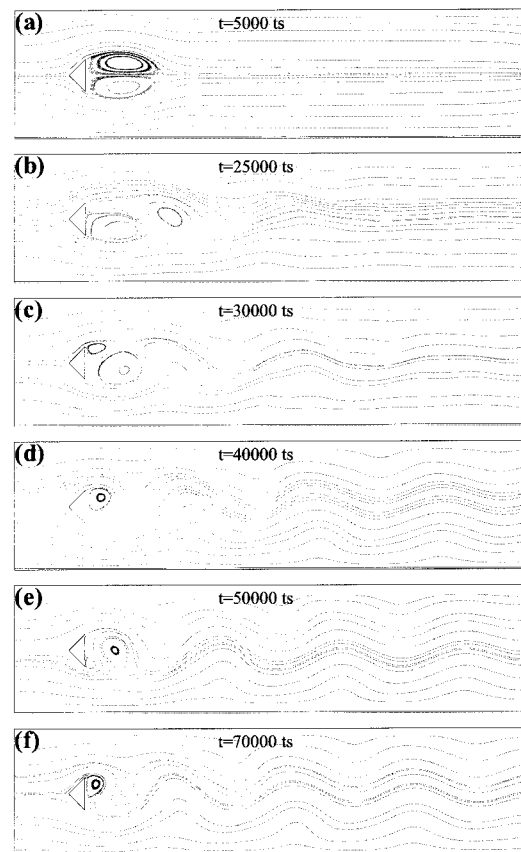


Fig. 5 Streamlines plot in x-y plane for different times

From the first plot, it is seen that the alternating vortices with same size and strength are shed from the upper and lower corner of the body. The flow pattern is symmetric for different time steps with respect to the oncoming flow and there is a closed recirculation zone just behind the body. This zone is made up of two symmetrical vortices that rotate in opposite directions. The next plots (5(b)-(e)) have shown that the low pressure core of the fully developed

vortex has pulled away from the body and consequently another new one is forming and it is observed that the vortices are shed alternately with time steps. Finally the last plot, at time steps $t=70,000$, is nearly identical with the Fig.5(d). This evolutionary process is repeated approximately every 30,000 time steps. The same phenomenon has been seen that for flow over an airfoil at -90 degree angle of attack documented by Rogers and Kwak¹¹⁾. In addition, if we increase the Reynolds number, the time period becomes shorter. It is investigated that, for $Re=200$, the time period is approximately about 15,000 time steps.

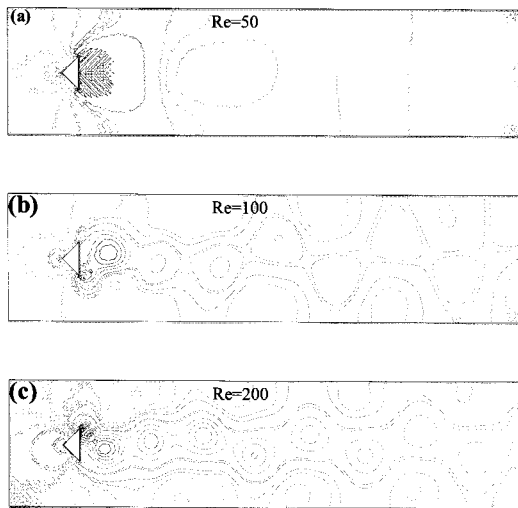


Fig. 6 Pressure field for flow across wedge - shaped bodies with different Re

Apart from the velocity profile, pressure distribution is important to understand the flow field behavior around the bluff bodies. Fig.6 shows the pressure contours with $Re=50$, 100 and 200. For lower Reynolds number, the variation of pressure contours are not significant at the far from the body. However for higher Reynolds number, it was more significant and the pressure contours becomes more complex and unstable. This is expected because by increasing the Reynolds number, the vortices become stronger. Stronger vortices cause low pressure in the wake and there exist maximum low pressure at the center of each vortex.

4. Conclusion

The present investigations provided us some important information regarding flow in the wake behind the wedge-shaped body with wedge angle $\Theta=90^\circ$. It has been seen that the vortex shedding frequency increases with the Reynolds number in the range up to $32 \leq Re \leq 620$. For lower Reynolds number ($=50$) the flow patterns were almost symmetric whereas for higher Reynolds number ($=100, 200$), the flow behind the body is characterized by a Karman vortex street, which consists of vortices in a regular arrangement. This phenomenon is seen after $Re \geq 85$. The distance between consecutive vortices remains almost constant. This distance as well as the time period becomes shorter with the increasing of Reynolds number. The time period for $Re=100$ is investigated approximately 30,000 time steps, whereas for $Re=200$, it observed about 15,000 time steps. Consequently the similar behaviors have been observed in pressure contours. Actually, the present study with LBM provides us a reliable and accurate results for 2D channel flow around a bluff body. Therefore, it gives us confidence to expand the application of LBM for the simulation at more complex fluid flow problems.

References

1. G. R. McNamara and G. Zanetti, 1988, "Use of the Boltzmann equation to simulate lattice-gas automata", *Physical Review Letters*, Vol 61, pp. 2332~2335.
2. H. Chen, S. Chen and W. H. Matthaeus, 1992, "Recovery of the Navier-Stokes equations using a lattice-gas Boltzmann method", *Physical Review A*, Vol. 45 No. 8, pp. 5339~5342.
3. Y. Qian, H. D. D'Humieres and P. Lallemand, 1992, "Lattice BGK models for Navier-Stokes equation", *Euro physics Letter*, Vol. 17, No. 6, pp. 479~484.

4. S. Chen and G. D. Doolen, 1998, "Lattice Boltzmann method for fluid flows", *Annu. Rev. Fluid Mechanics*, Vol. 30, pp. 329~364.
5. S. Succi, 2001, "The lattice Boltzmann equation for fluid dynamics and beyond" Oxford University press.
6. M. C. Sukop and D. T. Thorne, 2006, "Lattice Boltzmann modeling, An introduction for geoscientist and engineering", Springer. Heidelberg.
7. C. H. K. Williamson, 1988, "Defining a universal and continuous Strouhal - Reynolds number relationship for a laminar vortex shedding of a circular cylinder", *Physics of Fluid*. Vol. 31, No. 10, pp. 2742~274.
8. D. L. Young, J. L. Huang and T. I. Eldho, 2001, "Simulation of laminar vortex flow past cylinders using a coupled BEM and FEM model", *Comput. Methods Appl. Mecha. Engg.*, Vol. 190, pp. 5975~5998.
9. An-B. Wang, Z. Travnicek, and K-C. Chia, 2000, "On the relationship of effective Reynolds number and Strouhal number for the laminar vortex shedding of a heated circular cylinder", *Physics of fluid*, Vol. 12, No. 6, pp. 1401~1410.
10. P. J. Strykowski and K. R. Sreenivasan, 1990, "On the formation and suppression of vortex 'shedding' at low Reynolds numbers", *J. Fluid Mechanics*, Vol. 21B, pp. 71~107.
11. S. E. Rogers, and D. Kwak, 1990, "Up wind differencing scheme for the time-accurate incompressible Navier-Stokes equations", *AIAA Journal*, Vol. 28, No. 2, pp. 253~262.